Single Antenna Power Measurements Based Direction Finding

Joni Polili Lie, *Member, IEEE*, Thierry Blu, *Senior Member, IEEE*, and Chong Meng Samson See, *Member, IEEE*

Abstract—In this paper, the problem of estimating direction-of-arrival (DOA) of multiple uncorrelated sources from single antenna power measurements is addressed. Utilizing the fact that the antenna pattern is bandlimited and can be modeled as a finite sum of complex exponentials, we first show that the problem can be transformed into a frequency estimation problem. Then, we explain how the annihilating filter method can be used to solve for the DOA in the noiseless case. In the presence of noise, we propose to use Cadzow denoising that is formulated as an iterative algorithm derived from exploiting the matrix rank and linear structure properties. Furthermore, we have also derived the Cramér–Rao Bound (CRB) and reviewed several alternative approaches that can be used as a comparison to the proposed approach. From the simulation and experimental results, we demonstrate that the proposed approach significantly outperforms other approaches. It is also evident from the Monte Carlo analysis that the proposed approach converges to the CRB.

Index Terms—Annihilating filter, denoising, direction-of-arrival, single antenna direction finding.

I. INTRODUCTION

DIRECTION finding (DF) for multiple narrowband far-field signal sources has been discussed intensively in the literature. Early works exploit the directional radiation pattern characteristics to estimate the direction-of-arrivals (DOAs) of the signal sources by searching for the direction where the maximum signal level is obtained. Such techniques have a limited capability of resolving closely-spaced sources. Later on, the well-known multiple signal classification (MUSIC) algorithm is proposed as high-resolution DF. Instead of using single directional antenna, it estimates the DOAs from a vector of received signals at an antenna array [1], [2].

Although it is able to provide high-resolution DF, the MUSIC algorithm requires a computationally demanding spectral search procedure. To overcome this, search-free variants of the MUSIC algorithm are proposed. For examples, Root-MUSIC [3], ESPRIT [4] and their extensions [5], [6]. Besides the spectral search requirement, it is also highly sensitive to array model errors [7]–[9]. This drawback motivates the

use of robust techniques in order to recover the high resolution performance [10]–[13]. Other issues that are recently addressed also include the extension to arbitrary array geometry [14] and array calibration [15]–[17].

Despite the efforts on overcoming the drawbacks of the MUSIC algorithm, practical implementation is still challenging due to the multichannel receiver requirements [18]. This motivates the authors in [19]–[21] to consider DF methods using single-channel receiver. The key idea is to utilize the switched parasitic elements connected to an antenna array in order to construct multiple steerable beam. The DOAs can then be estimated from the steering direction that resulted in maximum signal level. Another recent single-channel DF approach exploits the fact that the convolution between the antenna radiation pattern and the DOA indicator function results in the received signal at different rotating direction [22], [23]. As such, the DOA indicator function can be obtained through deconvolution process from the spatial sounding measurement vector.

In this paper, we propose a single-antenna power measurements based DF technique that estimates the DOA from a vector of power measurements. It exploits the diversity in the antenna radiation pattern that is captured through the received power calculated when the antenna is pointing at different directions. From a vector of power measurements, the approach first utilizes a linear transformation of the power vector into a vector of spectral observations. The DOAs are then estimated as the solution to the spectral analysis. Due to the similarity of the approach to the finite-rate-of-innovation (FRI) sampling [24], the approach can be seen as performing spatial sampling of stream of Diracs whose locations are the DOAs.

The proposed approach belongs to the high-resolution DF approaches due to its ability to resolve two signal sources that are separated less than a beamwidth apart [25]. Besides the high resolution capability, the approach does not require any spectral search and is theoretically able to resolve as many sources as half the number of power measurements. Since it is not based on antenna array, the issues on array geometry and modeling error are not under consideration. Hence, it is very attractive from the practical implementation perspective.

II. SIGNAL MODEL AND PROBLEM STATEMENT

Notations

The following notations will be used in this paper:
- matrices (uppercase letters) and vectors (lowercase letters) are denoted by bold font;
- the ijth element of a matrix $\mathbf{A}$ is $\mathbf{A}_{ij}$, and $(\mathbf{A}_{i:}, \mathbf{A}_{:j})$ are the ith row vector and jth column vector of a matrix $\mathbf{A}$;

- diag{$\mathbf{A}$} denotes the diagonal elements of matrix $\mathbf{A}$ and Re{$\mathbf{A}$} denotes the real component of matrix $\mathbf{A}$; likewise, Im{$\mathbf{A}$} for the imaginary component;
- the superscripts $*, T, H, \dagger$ denote the conjugate, transpose, conjugate transpose, and pseudo-inverse operation respectively;
- $f * g$ means the convolution of f and g.

A. Signal Model

We consider a single antenna receiving system with the capability to calculate the power from the received signal. Given that the spatial response of the antenna is non-uniform, the received signal can be modeled as a sum of all the transmitted signal attenuated with direction-dependent factor. In mathematical form, the received signal $x(t)$ can be expressed as

$$x(t) = \sum_{k=1}^{K} g(\tilde{\theta} - \theta_k)s_k(t) + \eta(t)$$

where $g(\tilde{\theta} - \theta_k)$ is the antenna attenuation for the signal impinging from θ_k direction when the orientation of the antenna is at $\tilde{\theta}$, $s_k(t)$ is the kth impinging signal, $\eta(t)$ is the receiver's noise and K is the number of impinging signals. When the orientation of the antenna is no longer fixed, the received signal experiences different attenuations. Let $x_l(t)$ denote the received signal when the orientation is at $\tilde{\theta}_l$

$$x_l(t) = \sum_{k=1}^{K} g(\tilde{\theta}_l - \theta_k)s_k(t) + \eta(t).$$

The received signal power averaged over a duration T, in which the sources of impinging signals $s_k(t)$ are assumed to be stationary, can then be approximated as

$$p_l = \frac{1}{T} \int_T x_l^2(t) dt \approx \sum_{k=1}^{K} \underbrace{|g(\tilde{\theta}_l - \theta_k)|^2}_{a(\tilde{\theta}_l - \theta_k)} r_k + n_l \quad (1)$$

where

$$r_k = \frac{1}{T} \int_T |s_k(t)|^2 dt, \quad \text{and} \quad n_l = \frac{1}{T} \int_T |\eta(t)|^2 dt.$$

This approximation is valid under the assumption that the impinging signals are uncorrelated, hence the cross term is negligible:

$$\int_T g(\tilde{\theta}_l - \theta_{k_1})g(\tilde{\theta}_l - \theta_{k_1})s_{k_1}(t)s_{k_2}(t) dt \approx 0, \quad k_1 \neq k_2.$$

Hence, the problem considered here can be stated as follows: given a vector of the received power $\mathbf{p} = [p_1, \ldots, p_L]^T$ measured when the sources of $s_k(t)$ are in stationary condition, the objective is to estimate the direction-of-arrival (DOA) of the impinging signals, $\boldsymbol{\theta} = [\theta_1, \ldots, \theta_K]^T$.

B. Antenna Pattern and Power Estimation Model

Let $a(\theta)$ denote the spatial power response of the antenna (also known as antenna pattern). We have observed that it can be well approximated (see Section VII) as a finite sum of complex exponentials[1] according to

$$a(\theta) = \sum_{m=-M}^{M} a_m e^{jm\theta} \quad (2)$$

where M is some finite integer. Notice that because $a(\theta)$ is a real-valued function, the model in (2) is valid if $a_m = a_{-m}^*$. Also, the antenna pattern is a 2π-periodic non-negative function $a(\theta) = a(\theta + 2\pi)$ and $a(\theta) \geq 0, \forall \theta$.

In calculating the power of the received signal, the following power estimation formula is used

$$\hat{p}_l = \frac{1}{N} \sum_{n=1}^{N} |x_l(n)|^2 \quad (3)$$

where N is the number of snapshots and $x_l(n)$ is the nth discrete sample of the received signal $x_l(t)$. Note that although the power is estimated from the discrete sample of the received signal, only the vector of average power measurements is assumed to be known. Thus, the received signal is not available. This constraint is required in order to realize a low-complexity low-cost direction finder. However, the power estimation formula is necessary for numerical analysis and in deriving Cramér–Rao Bound of the estimation problem (as detailed in Section IV).

III. PROPOSED APPROACH

A. Transformation Into Spectral Analysis Problem

Substitute (2) into the received power expression in (1)

$$\begin{aligned} p_l &= \sum_{k=1}^{K} \sum_{m=-M}^{M} a_m e^{jm(\tilde{\theta}_l - \theta_k)} r_k + n_l \\ &= \sum_{m=-M}^{M} \underbrace{\sum_{k=1}^{K} r_k e^{-jm\theta_k}}_{y_m(\boldsymbol{\theta})} a_m e^{jm\tilde{\theta}_l} + n_l \end{aligned}$$

and we can formulate a matrix equation in the linear form

$$\mathbf{p} = \mathbf{A}\mathbf{y}(\boldsymbol{\theta}) + \mathbf{n}-$$

using the following matrix and vectors definitions: $\mathbf{n} = [n_1, \ldots, n_L]^T$ are real-valued vectors of size L, $\mathbf{y}(\boldsymbol{\theta}) = [y_{-M}(\boldsymbol{\theta}), \ldots, y_M(\boldsymbol{\theta})]^T$ is a complex-valued vectors of size $2M + 1$ and $\mathbf{A}$ is a $L \times (2M + 1)$ matrix with its element given by

$$\mathbf{A}_{lm} = a_m e^{jm\tilde{\theta}_l}.$$

The vector $\mathbf{y}(\boldsymbol{\theta})$ can be retrieved from the vector of received power when $L \geq 2M + 1$ using the least-square estimation formula as follows:

$$\hat{\mathbf{y}}(\boldsymbol{\theta}) = \mathbf{A}^{\dagger}\mathbf{p} \quad (4)$$

where the superscript $\dagger$ denotes pseudo-inverse operation.

---

[1]Such a decomposition of the antenna pattern has been extensively studied in the literature, and its bandwidth has been shown to be limited by the calibration noise; see, e.g., [26]–[30].

In the case where the antenna is oriented in a regular and uniform manner, that is

$$\tilde{\theta}_l = \tilde{\theta}_0 + l\alpha$$

we will see that the retrieval of the angles θ_k is analogous to a frequency estimation problem, typical of FRI settings [24], [31]. When $\alpha = 2\pi/L$, $\mathbf{A}^\dagger$ is actually a simple inverse DFT. Instead of sampling in time, the system considered here is performing spatial sampling using the power measurements taken from different spatial orientation. Also, the sampling kernel used here is the antenna pattern. Hence, the problem can also be translated into spatial sampling with finite rate of innovation where the sampling interval is non-uniform.

B. Annihilating Filter

Recall that y_m is a sum of K exponentials

$$y_m = \sum_{k=1}^{K} r_k e^{-jm\theta_k}. \tag{5}$$

To obtain $\boldsymbol{\theta}$, it is possible to find a filter of length $K+1$ with coefficients h_m such that $h_m * y_m = 0$. This filter is termed as annihilating filter.

The z-transform of this filter is given by

$$H(z) = \text{Const} \times \prod_{k=1}^{K} (1 - z_k z^{-1})$$

where the polynomial roots z_k contains the DOA information θ_k because

$$z_k = e^{-j\theta_k}.$$

To find the coefficients h_m from y_m, we solve

$$\min_{h_m} \sum_m |h_m * y_m|^2 \quad \text{subject to} \quad \sum_m |h_m|^2 = 1.$$

The solution can be obtained by computing the singular value decomposition (SVD) of a Toeplitz matrix built using y_m. Then, the polynomial roots of $H(z)$ is solved from the coefficients h_m and the DOAs can be calculated by

$$\hat{\theta}_k = -j \log(z_k). \tag{6}$$

The DOA estimate will be ranging from $-\pi$ to π, that is, $-180° < \hat{\theta}_k \leq 180°$. The negative values refer to the directions greater than $180°$. Therefore, the estimate can be adjusted by first adding 2π and then taking the modulo-2π. The resulting value will be ranging from $0°$ to $360°$.

It is important to note that the above approach is capable of resolving any pair of closely-spaced sources for the *noiseless* case. In other words, there is no limitation in the DF resolution. Nevertheless, the number of resolvable DOAs is limited by the parameter M. This is related to the bandwidth requirement for the sampling kernel in the FRI sampling problem. The bandwidth of the antenna pattern with the model in (2) is $2M + 1$. Thus, it is able to estimate M DOAs accurately.

However, this is not the case in practice because the received signal is noisy. The estimation will lose its accuracy due to the noise. As explained next, this can be overcome with denoising algorithm which requires the parameter M to be greater than the number of sources K. The larger the parameter M, the better the estimation accuracy.

C. Cadzow Denoising

Because the received power is calculated from the noisy measurements of the received signal, $\hat{y}_m$ will be subjected to an estimation error. Hence, as the noise power from the received signal increases, the annihilating filter coefficients h_m will not yield a good estimate of the DOAs.

To overcome this, it is necessary to include a denoising algorithm to denoise $\hat{y}_m$ [31]. Cadzow in [32] proposes a composite property mapping algorithm that exploits the signal attributes and properties of matrix representation to perform denoising. We first show that the Toeplitz matrix built from y_m also possesses the similar attributes and properties as those exploited in Cadzow denoising algorithm. Then, we discuss the implementation of the denoising algorithm.

Let $\hat{\mathbf{Y}}$ denote the Toeplitz matrix of size $(2M - J + 1) \times (J + 1)$, constructed from the element of $\hat{y}_m$ as follows:

$$\hat{\mathbf{Y}} = \begin{bmatrix} \hat{y}_{-M+J} & \hat{y}_{-M+J-1} & \cdots & \hat{y}_{-M} \\ \hat{y}_{-M+J+1} & \ddots & \ddots & \vdots \\ \vdots & \ddots & \ddots & \vdots \\ \vdots & & \ddots & \hat{y}_{M-J-1} \\ \hat{y}_M & \cdots & \hat{y}_{M-J+1} & \hat{y}_{M-J} \end{bmatrix}. \tag{7}$$

The first property of the matrix is the matrix rank. Because y_m is modeled as sum of K exponent terms given in (5), the rank of the Toeplitz matrix constructed from y_m according to (7) will be equal to K. Using this rank property, it is possible to *denoise* the Toeplitz matrix $\hat{\mathbf{Y}}$ by using rank reduction mapping. This matrix mapping function can be written as follows:

$$\hat{\mathbf{Y}}^{(K)} = F^{(K)}(\hat{\mathbf{Y}}) = \sum_{k=1}^{K} \lambda_k \mathbf{u}_k \mathbf{v}_k^H \tag{8}$$

where $\{\lambda_1, \ldots, \lambda_K\}$ are K largest eigenvalues and the unitary vectors $(\mathbf{u}_k, \mathbf{v}_k)$ are the K vectors associated to the K eigenvalues. These vectors can be obtained through SVD. Alternatively, this matrix mapping can be seen as reconstructing the Toeplitz matrix from *only K eigen-components*. It is worth mentioning that this mapping requires the number of sources K to be known. Otherwise, it can be estimated using the information theoretic criterion methods, e.g., MDL or AIC [33].

The second property is the linear structure property. This property can be shown by utilizing a matrix reordering function. Let $T(\cdot)$ denote the matrix reordering function that reshapes a matrix into a column vector. The reordering can be explained as follows:

$$T(\hat{\mathbf{Y}}) = [\hat{\mathbf{Y}}_{:1}^T \quad \hat{\mathbf{Y}}_{:2}^T \quad \cdots \quad \hat{\mathbf{Y}}_{:(J+1)}^T]^T.$$

After the reordering, the resulting vector can be modeled as overdetermined linear system of equations

$$T(\hat{\mathbf{Y}}) = \mathbf{S}\hat{y}(\boldsymbol{\theta})$$

where $\mathbf{S}$ is a selection matrix with elements 0s and 1s. Thus, by utilizing the linear structure property, the denoising of $\hat{\mathbf{Y}}$ can be realized by taking a least squares estimate of $\hat{\mathbf{y}}(\boldsymbol{\theta})$ and followed by inverse reordering to reshape back into a matrix representation. These operations form another matrix mapping function

$$\hat{\mathbf{Y}}^{\text{LS}} = F^{\text{LS}}(\hat{\mathbf{Y}}) = T^{-1}(\mathbf{S}^{\dagger}T(\hat{\mathbf{Y}})). \tag{9}$$

By combining both matrix mapping function in (8) and (9), an iterative composite mapping algorithm for denoising of $\hat{\mathbf{Y}}$ can be constructed using the following composite mapping function

$$F(\hat{\mathbf{Y}}) = F^{\text{LS}}(F^{(K)}(\hat{\mathbf{Y}})). \tag{10}$$

After a few iterations, the denoising algorithm will provide a good approximation of a rank-K Toeplitz matrix. This can be seen from the value of the eigenvalues $\{\lambda_{K+1}, \lambda_{K+2}, \ldots\}$: as iteration continues, these eigenvalues approaches zero. As will be demonstrated via numerical experiments in Section VI, the accuracy of the estimator improves as the iteration converges.

As stated in [32], the convergence of the Cadzow denoising requires that the composite property mapping of $\hat{\mathbf{Y}}$ in (10) be a closed mapping. It has also been proven in [32] that the composite mapping is a closed mapping. Hence, it can be concluded that the Cadzow denoising algorithm converges.

D. Summary of Proposed Approach

In summary, the proposed approach for estimating $\boldsymbol{\theta}$ given the vector of power measurements $\mathbf{p}$ can be listed as follows.
1) Estimate $\hat{\mathbf{y}}(\boldsymbol{\theta})$ using (4).
2) Form a Toeplitz matrix $\hat{\mathbf{Y}}$ from $\hat{\mathbf{y}}(\boldsymbol{\theta})$ using (7). The column size of the Toeplitz matrix can be arbitrarily set to a value larger than K but not greater than $M+1$.
3) *Denoising*: Run (10) for 20 iterations.
4) Compute the annihilating filter coefficients h_m from the $K+1$ eigenvectors of the denoised $\hat{\mathbf{Y}}$. This requires SVD or eigen-decomposition of $\hat{\mathbf{Y}}$.
5) Find the polynomial roots of the annihilating filter z_k from the coefficients h_m.
6) The estimate of $\boldsymbol{\theta}$ can be calculated from z_k using (6).

IV. CRAMÉR–RAO BOUND

In this section, we will derive the Cramér–Rao bound (CRB) of the estimator. Previous work reported by Porat and Friedlander [34] and subsequently adapted by Blu *et al.* [31] includes the derivation of the CRB when the noise is additive. In the problem presented in this paper, the noise appearing in the received power is calculated from the finite sum of squares of the received signal. Firstly, we will investigate the noise transformation from the power calculation to the estimation of $y_m(\boldsymbol{\theta})$. By showing that the estimation error can be approximated as Gaussian distribution, we will then deduce the CRB expression for $\boldsymbol{\theta}$.

A. Noise Transformation Analysis

To assess the proposed estimation, it is important to know the noise distribution. We start by assuming that the discrete samples of the receiver's noise $\eta(n)$ are complex-valued white Gaussian random variables with zero mean. That is,

$$\eta(n) \sim \mathcal{CN}(\mu_{\eta}, \Gamma_{\eta}, C_{\eta}) \tag{11}$$

where $\mu_{\eta} = 0$, $\Gamma_{\eta} = 2\sigma^2$, $C_{\eta} = 0$ and $\mathcal{CN}$ denotes complex normal distribution random variable.

Given that the received power can be estimated from the discrete samples of the received signal using the expression in (3), the noise at the received power is distributed according to (see Appendix A for a detailed derivation)

$$\hat{p}_l \sim \mathcal{N}(\mu_{\hat{p}_l}, \sigma_{\hat{p}_l}^2)$$
$$\mu_{\hat{p}_l} = \frac{1}{N} \sum_{n=1}^{N} \left| \sum_{k=1}^{K} g(\tilde{\theta}_l - \theta_k) s_k(n) \right|^2 + 2\sigma^2$$
$$\sigma_{\hat{p}_l}^2 = \frac{4\sigma^4}{N}. \tag{12}$$

Recall that from the L estimates of the received power, the proposed approach transforms the problem into a spectral analysis problem using the matrix multiplication in (4). Because the matrix multiplication can be seen as a linear transformation of a vector of random variable, we can therefore devise the distribution of the vector $\hat{\mathbf{y}}$ as expressed in (4) with $\hat{\mathbf{p}}$ constructed from L elements of $\hat{p}_l$. Since $\hat{\mathbf{p}}$ follows a multivariate normal distribution, we know that its linear combination will also follow a multivariate normal distribution. Therefore, we have

$$\hat{\mathbf{p}} \sim \mathcal{N}_L(\boldsymbol{\mu}_p, \boldsymbol{\Sigma}_p)$$
$$\boldsymbol{\mu}_p = [\mu_{\hat{p}_1}, \ldots, \mu_{\hat{p}_L}]^T$$
$$\boldsymbol{\Sigma}_p = \text{diag}\{[\sigma_{\hat{p}_1}^2, \ldots, \sigma_{\hat{p}_L}^2]\} \tag{13}$$

and we can obtain the distribution of $\hat{\mathbf{y}}$

$$\hat{\mathbf{y}} \sim \mathcal{N}_{2M+1}(\boldsymbol{\mu}_y, \boldsymbol{\Sigma}_y)$$
$$\boldsymbol{\mu}_y = \mathbf{A}^{\dagger} \boldsymbol{\mu}_p$$
$$\boldsymbol{\Sigma}_y = (\mathbf{A}^{\dagger}) \boldsymbol{\Sigma}_p (\mathbf{A}^{\dagger})^H. \tag{14}$$

With the expression in (14), we can then proceed to derive the Cramér–Rao bound as discussed next.

B. CRB Derivation

From the distribution of $\hat{\mathbf{y}}$, we can rewrite the signal model as

$$\hat{\mathbf{y}} = \mathbf{Q}\mathbf{r} + \mathbf{e} \tag{15}$$

using the following matrix and vectors definition: $\mathbf{r} = [r_1, \ldots, r_K]^T$, $\mathbf{e} = [e_{-M}, \ldots, e_M]$ and

$$\mathbf{Q} = [\mathbf{q}_1 \quad \cdots \quad \mathbf{q}_K]$$
$$\mathbf{q}_k = [e^{-jM\theta_k} \quad \cdots \quad 1 + 2\sigma^2 \quad \cdots \quad e^{jM\theta_k}]^T.$$

Notice that the $\{m = 0\}$th element of $\mathbf{q}_k$ has a biased term $2\sigma^2$. This term will not affect the estimator because it is not a function of $\boldsymbol{\theta}$. The noise vector $\mathbf{e}$ is a multivariate Gaussian distribution

$$e_m \sim \mathcal{N}(\mathbf{0}, \boldsymbol{\Sigma}_y).$$

For brevity of notation, let $\bar{M} = 2M + 1$. The likelihood function of the vector $\hat{\mathbf{y}}$ is given by

$$L(\hat{\mathbf{y}}) = \frac{1}{(2\pi)^{\bar{M}/2}|\boldsymbol{\Sigma}_y|^{1/2}}$$
$$\times \exp\left(-\frac{1}{2}[\hat{\mathbf{y}} - \mathbf{Qr}]^H \boldsymbol{\Sigma}_y^{-1}[\hat{\mathbf{y}} - \mathbf{Qr}]\right).$$

The CRB can be derived following the derivation in [35]. In fact, given the signal model in (15), our CRB can be seen as the extension of the CRB derivation in [35] with the noise vector being a multivariate normal distribution random vector:

$$\mathrm{CRB}^{-1}(\boldsymbol{\theta}) = 2\,\mathrm{Re}\left\{\mathrm{diag}[\mathbf{r}]^H \mathbf{D}^H \boldsymbol{\Sigma}_y^{-1} \mathbf{P}_{\mathbf{Q}}^{\perp} \mathbf{D}\,\mathrm{diag}[r]\right\} \quad (16)$$

where $\mathbf{P}_{\mathbf{Q}}^{\perp} = \mathbf{I} - \mathbf{Q}(\mathbf{Q}^H\mathbf{Q})^{-1}\mathbf{Q}^H$ and the mkth element of matrix $\mathbf{D}$ is given by

$$\mathbf{D}_{mk} = \frac{d}{d\theta_k}\mathbf{Q}_{mk} = jme^{jm\theta_k}.$$

Hence, one can refer to [35] for a detailed derivation of CRB. In general, the same CRB expression will be obtained if the bias term $2\sigma^2$ is not present at the signal model.

V. ALTERNATIVE APPROACHES

Besides transforming into a spectral analysis problem, it is possible to approach the problem in an alternative way as described in this section. Firstly, we define a vector whose elements are composed of sufficiently fine grid of DOAs: $\boldsymbol{\vartheta} = [\vartheta_1, \ldots, \vartheta_G]^T$, where G denotes the number of DOAs that define the grid. Then, the L-dimension vector of the received power can be expressed in an alternative linear form given by

$$\hat{\mathbf{p}} = \boldsymbol{\Phi}(\boldsymbol{\vartheta})\mathbf{d} + \mathbf{n} \quad (17)$$

where $\mathbf{d} = [d_1, \ldots, d_G]^T$ is a sparse vector consisting of $(G - K)$ elements of zeros and K elements of $\{r_1, \ldots, r_K\}$ and

$$\boldsymbol{\Phi}_{lg} = a(\tilde{\theta}_l - \vartheta_g).$$

With this reformulation, we can deduce a basic least squares (LS) approach from minimizing the least squares error

$$\min_{\mathbf{d}} \|\boldsymbol{\Phi}(\boldsymbol{\vartheta})\mathbf{d} - \hat{\mathbf{p}}\|_2^2.$$

The DOAs $\boldsymbol{\theta}$ can be estimated from K largest elements of the sparse vector estimate, $\hat{\mathbf{d}}$, obtained from solving the LS minimization.

Since the non-zero elements of $\mathbf{d}$ are the received power of individual transmission and they are *strictly* positive, it is possible to impose a non-negative constraint into the LS minimization. This optimization is still solvable and can be written as

$$\min_{\mathbf{d}} \|\boldsymbol{\Phi}(\boldsymbol{\vartheta})\mathbf{d} - \hat{\mathbf{p}}\|_2^2 \quad \text{s.t.} \quad \mathbf{d} \geq 0. \quad (18)$$

The solution to this optimization is known as non-negative least squares (NNLS) solution [36]. Similar to LS solution, the DOA estimation is achieved by searching for K largest elements of the NNLS solution. However, unlike the LS solution, there is no closed-form solution for the NNLS solution. The implementation of the NNLS solution requires an iterative algorithm.
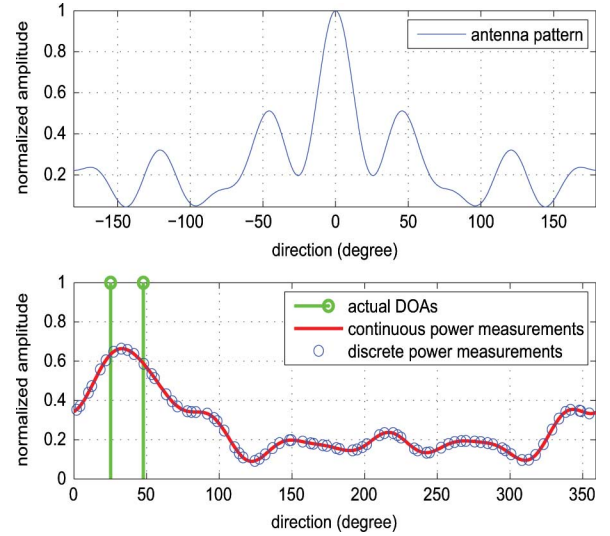
Fig. 1. (a) An example of the realization of antenna pattern simulated according to (2) with $M = 9$. (b) The power level versus the direction plotted with the actual DOA locations indicated by '—o'.

As compared to the proposed approach described in Section III, the resolution of the DOA estimation based on these approaches are limited by the resolution of the DOA grid defined by $\boldsymbol{\vartheta}$. Besides least squares based approaches, the solution based on minimization of ℓ_1-norm can also be considered from the same signal model in the form (17). Due to the high measure of sparsity, the solution based on ℓ_1-norm minimization may yield a better estimate [37]. Nonetheless, this approach shares the same limitation as the least squares based approach.

VI. SIMULATION RESULTS

We consider a directional antenna with the antenna pattern simulated using the expression $g(\theta) = \sum_{m=0}^M g_m e^{jm\theta}$ with $M = 9$ and $\{g_m, m \in \{1, \ldots, M\}\}$ generated randomly according to uniform distribution. Then, the g_0 is set such that the antenna pattern is a nonnegative function. Fig. 1(a) shows an example of the antenna pattern.

The propagation environment is simulated such that two uncorrelated sources emitting from $25.208°$ and $47.7191°$. When arrived at the receiving antenna, it is modeled as

$$s_k(n) = \sqrt{\alpha_k}\exp(j[2\pi f_k n + \varphi_k])$$

with the parameters set as: $\alpha_k = [0.9, 0.8]$, $f_k = [0.253, 0.347]$, and $\varphi_k = [0.0136, 0.8044]$. It is important to note that although the simulations presented in this paper consider narrowband signal model, the proposed method does not require narrowband assumption and is able to process wideband signals centered at different frequencies. As many as $N = 512$ samples of the received signal are used to compute the received power and $L = 76$ values of the received power are collected from different antenna orientation generated randomly within $0°$ and $359°$. Fig. 1(b) shows the actual DOAs as well as the continuous and discrete power measurements that forms the vector $\mathbf{p}$ for the noiseless case. The DOAs are estimated from the discrete power measurements of the noisy case. Looking at the continuous power measurements plot, we can see that high resolution DF technique is required to resolve the two closely-spaced sources.
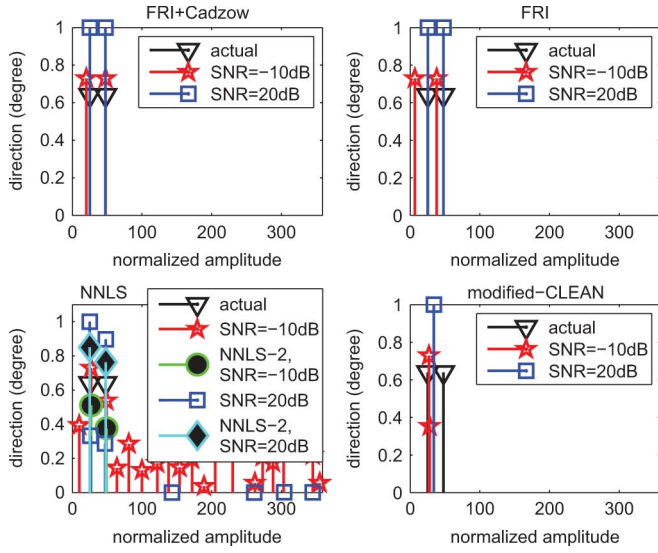
Fig. 2. DOA estimation result for $N = 512$, $L = 76$, and $\boldsymbol{\theta} = \{25.208°, 47.7191°\}$.

Fig. 3. DOA estimation result for $N = 512$, $L = 76$, and $\boldsymbol{\theta} = \{25.208°, 157.7191°\}$.

In our first simulation, we evaluate on five different DF methods and show how they resolve the two closely-spaced sources. They include the FRI method with and without the Cadzow denoising algorithm, as well as the NNLS method with and without the *prior* knowledge (on the number of sources K) and the deconvolution with modified CLEAN [23]. The FRI method is implemented according to the procedure listed in Section III-D with the Step 3) skipped for that without the Cadzow denoising. The column size of the Toeplitz matrix is set to $M + 1$ so that it becomes a square matrix. For the implementation of the deconvolution method with modified CLEAN, we use linear interpolation to obtain the continuous function of the received power from the 76 power measurements and then deconvolute it with the continuous antenna pattern before going through the modified CLEAN algorithm as proposed in [23]. The NNLS method with *prior* knowledge of K is implemented by keeping only K largest peaks.

Fig. 2 shows the stem-plot of the normalized amplitude against the corresponding DOA estimation results when signal-to-noise ratio (SNR) is set at -10 and 20 dB. The amplitudes shown are not the amplitudes retrieved: the apparent differences are only meant to make easier the viewing of the graphs. NNLS-2 refers to the NNLS method with *prior* knowledge on the number of signals. The same simulation setting is also used to generate Figs. 3, 12, 14, and 15. The SNR is calculated as the total power of the impinging signal at the antenna over the noise power[2]:

$$\text{SNR} = \frac{\left(\sum_{k=1}^{K} \alpha_k\right)}{2\sigma^2}.$$

Note that both the NNLS and the deconvolution with modified CLEAN method belong to the peak search based method. They require peak search procedure to identify the peak from

[2]The SNR expression here is calculated at the received signal $x(t)$.
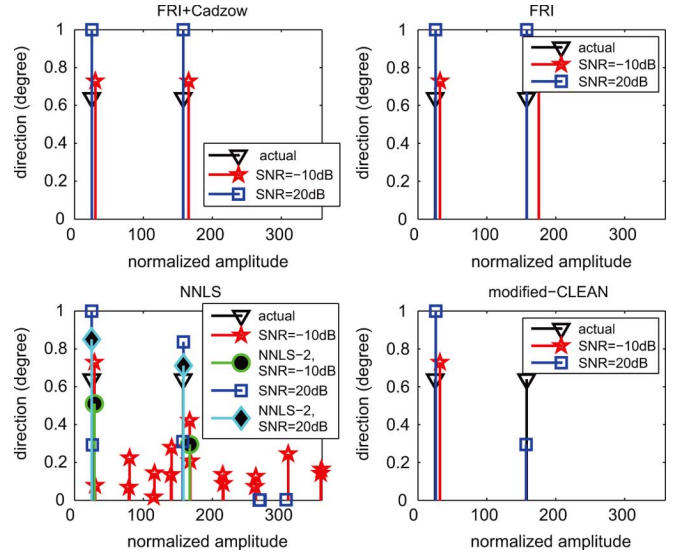
the DOA indicator function, while this is not the case for the FRI based method.

When SNR is low, the DOA indicator function from the NNLS method shows many spurious peaks. While this drawback is not observed in the deconvolution method, it is unable to resolve the two sources due to the close separation. Fig. 2 also demonstrates how our implementation of Cadzow denoising algorithm helps to recover the performance in the low SNR case.

Next, we simulate another realization by keeping all parameters unchanged except for the DOA of the sources. Instead of having two closely-spaced sources, we simulate the case when the two sources are well separated ($\theta_1 = 25.208°$ and $\theta_2 = 157.7191°$). In this case, we expect the deconvolution method to be able to resolve the two sources. Fig. 3 shows the normalized amplitude plot as a function of the DOA estimation results. As expected, like the other methods, the deconvolution method is able to resolve the two sources.

In the following simulation, we consider 1000 realizations and calculate the root mean-square error (RMSE) from the corresponding 1000 estimation results. Among the peak-search-based methods, only the NNLS-2 is compared against the FRI-based methods in this simulation. This is because the RMSE calculation for the deconvolution method becomes ambiguous when it only provides single DOA estimate. Hence, it is omitted in the following simulations. Fig. 4 shows the DOA estimation RMSEs of the FRI method with and without Cadzow denoising and the NNLS method with prior knowledge of K as a function of SNR. The square root of the CRB as derived in (16) is also shown. From this figure, it can be observed that the use of our Cadzow denoising significantly improves the performance. When the SNR is -5 dB or higher, the performance of the FRI method with Cadzow denoising converges to that of the lower bound. This can be explained due to the bandwidth of the antenna pattern used that allows the denoising algorithm to reduce the noise effect. In addition, we also evaluate the bias of the estimators as shown in Fig. 5. It is important to note that the
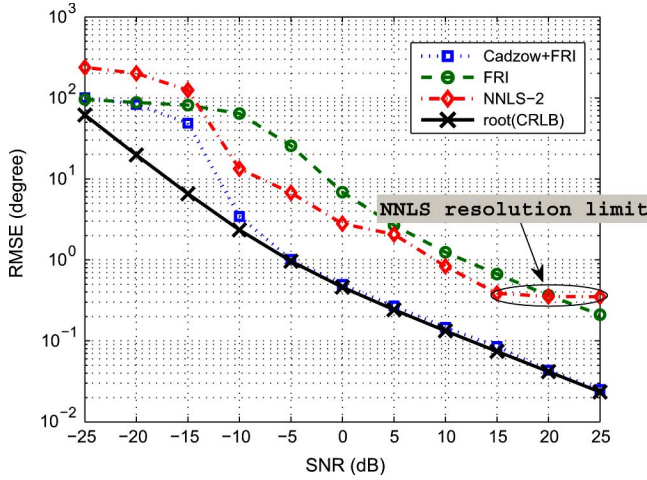
Fig. 4. DOA estimation RMSEs versus SNR for $N = 512$ and $\boldsymbol{\theta} = \{25.208°, 47.7191°\}$, obtained from $L = 26$ power measurements. The antenna pattern is modeled with $M = 11$.
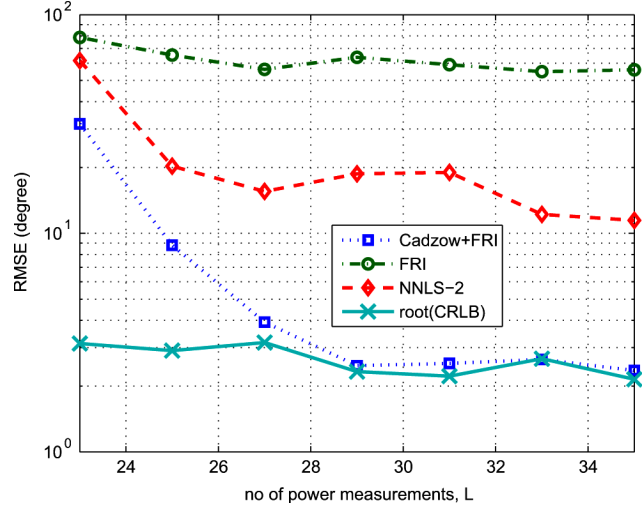
Fig. 6. DOA estimation RMSEs versus the number of power measurements for $N = 512$ and $\boldsymbol{\theta} = \{25.208°, 47.7191°\}$. The antenna pattern is modeled with $M = 11$ and the SNR is set at -10 dB.
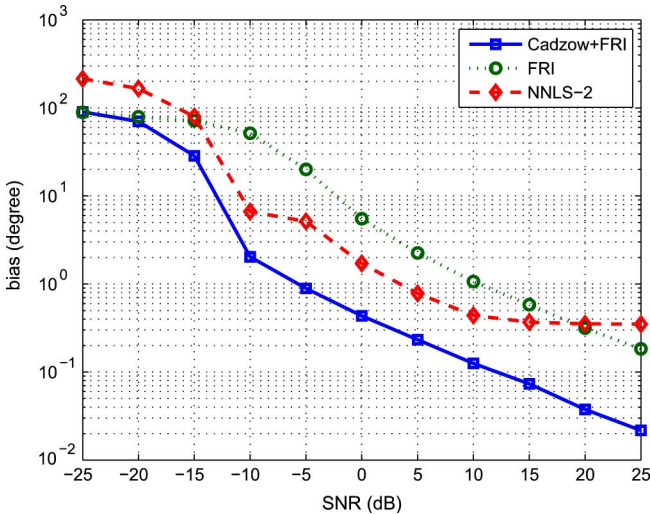
Fig. 5. DOA estimation bias versus SNR for $N = 512$ and $\boldsymbol{\theta} = \{25.208°, 47.7191°\}$, obtained from $L = 26$ power measurements. The antenna pattern is modeled with $M = 11$.
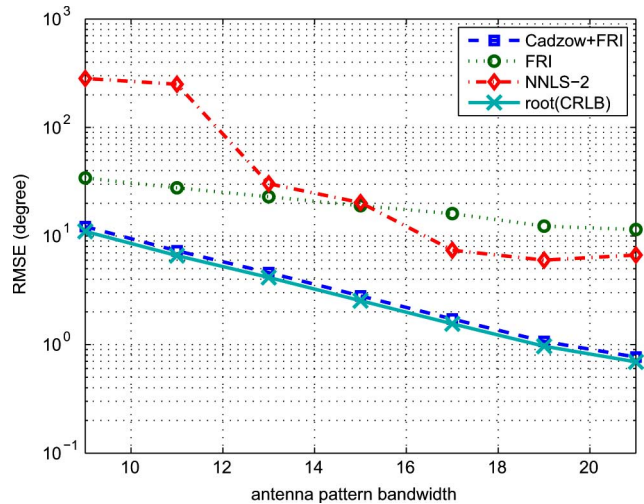
Fig. 7. DOA estimation RMSEs versus the antenna pattern bandwidth for $N = 512$, $L = 26$ and $\boldsymbol{\theta} = \{25.208°, 47.7191°\}$. The SNR is set at -5 dB.

NNLS-2 is implemented with 1° step-size. Therefore, its accuracy will be limited and this effect can be seen in Figs. 4 and 5 when $\mathrm{SNR} > 15$ dB.

Next, we fixed the SNR at -10 dB and vary the number of power measurements. The estimation results shown in Fig. 6 implies that taking more power measurements can help to further improve the estimation performance in low SNR environment.

The next simulation helps to validate the hypothesis that antenna pattern bandwidth affects the estimation performance through the denoising algorithm. We keep all the parameters unchanged except for the antenna bandwidth, which is varied by changing the parameter M. Fig. 7 shows the DOA estimation RMSEs versus the antenna pattern bandwidth. It clearly demonstrates that as the bandwidth increases, the RMSE performance of the proposed approach converges to the CRB.

The last two simulations examine the performance of the methods versus the angular separation between two sources

and the performances when the number of sources increases. Fig. 8 displays the DOA estimation RMSEs versus the angular separation simulated when the DOA of the first source is fixed at $25.208°$ while the second DOA is varied. M is set at 11 and all other parameters are chosen from the previous example. It can be seen clearly that the proposed approach is unable to converge to the CRB performance when the angular separation is less than $15°$. Theoretically, the approach has no limitation on the angular resolution. However, due to the presence of noise, the accuracy is affected. To illustrate this, we also simulate for the higher SNR case, i.e., $\mathrm{SNR} = 5$ dB. As clearly shown, the approach has better resolution for the higher SNR case.

Fig. 9 redisplays the RMSE plots versus SNR for $K = 2$ sources and compares them with the RMSE plots for $K = 4$. Given the same antenna pattern, the approach yields better performance for lesser sources in the low SNR case. This can be observed from the plots at -10 dB SNR. The approach achieves CRB performance for $K = 2$ while it is not the case for $K = 4$.
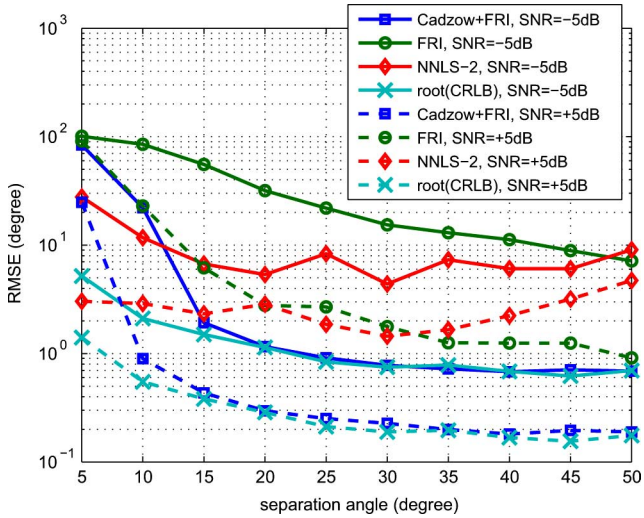
Fig. 8. DOA estimation RMSEs versus the angular separation for $N = 512$, $L = 26$, $M = 11$ and $\theta_1 = 25.208°$ while θ_2 is varied.
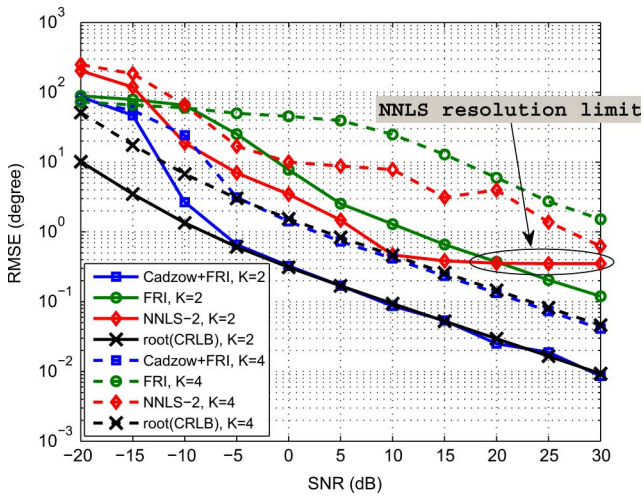
Fig. 9. DOA estimation RMSEs versus SNR for $N = 512$, $L = 26$, $M = 11$ and $\boldsymbol{\theta} = \{25.208°, 47.7191°\}$ for $K = 2$ sources and $\boldsymbol{\theta} = \{25.208°, 47.7191°, 75.4563°, 105.2431°\}$ for $K = 4$ sources.

Fig. 10. Schematic diagram of the direction finding receiver.
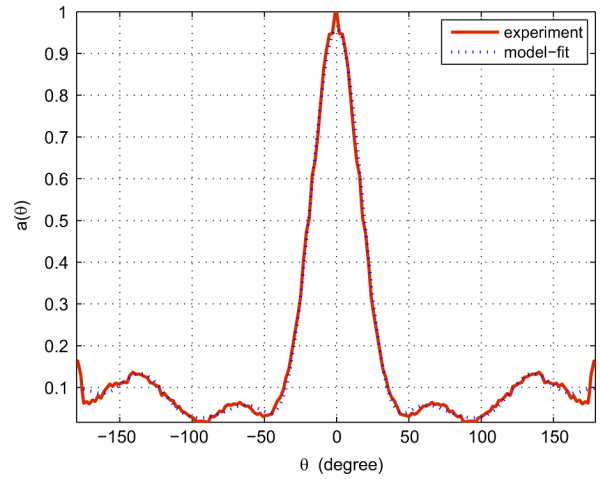
Fig. 11. Normalized antenna pattern plots of the GSM directional antenna. Solid line shows the plot obtained from the experimental results while the dotted line shows the plot obtained by fitting the solid-line curve using the polynomial model in (2) where $M = 8$.

VII. EXPERIMENTAL RESULTS

In this section, we present the results from experiments using the hardware realization of the proposed approach. Firstly, we explain the configuration of the DF receiver and the experimental setup in the DF experiments. Next, we describe the antenna pattern model obtained from the anechoic chamber experiment. And lastly, we show the results of the DF experiments conducted in three different propagation environments.

To realize the proposed DF receiver, we utilize the directional GSM antenna as shown in Fig. 10. To compute the received power, the received signal has to be first down-converted then sampled. To achieve that, we use winRadio RF-to-IF down-converter [38] and Red Rapids PCMCIA-based acquisition card [39]. The acquisition card is able to supply 14-bit discrete samples of the in-phase and quadrature phase of the analog signal. To measure the orientation of the antenna when the received signal is sampled, a digital compass OS5000-US manufactured by Ocean Server is utilized [40]. It can be connected to a USB

port and it streams 19200 baud rate data which consists of its orientation with respect to true north. As a whole, the schematic of the DF receiver can be shown in Fig. 10. Since the directional GSM antenna is operating in GSM band, we deploy GSM transmitters emitting single-tone sinusoidal wave at 900 MHz. A GSM transmitter comprises of an omnidirectional GSM antenna connected to a signal generator.

We first utilize single GSM transmitted placed in an anechoic chamber at the transmitting end while the DF received is placed at the receiving end. This experiment is conducted in order to acquire the antenna pattern of the GSM antenna. By taking power measurements for every $2°$ rotation, the normalized pattern can be shown in Fig. 11.

From the experimental pattern, we then try to fit the pattern to the sum of exponent terms model in (2) using least squares based regression technique by varying the parameter M. When $M = 8$, the residual is small enough such that increasing M only results in insignificant further reduction in the residual. Therefore, we select $M = 8$ and obtain the parameters g_m that best model the antenna pattern. The comparison between the antenna pattern from the experimental and that from the model-fitting is shown as well in Fig. 11.

Next, we conducted a single-source propagation experiment inside the anechoic chamber. Thirty-four power measurements
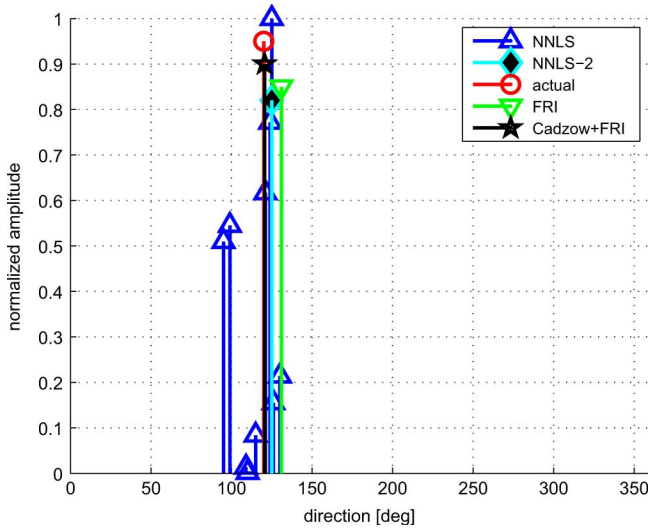
Fig. 12.   Experimental results from anechoic chamber experiment.
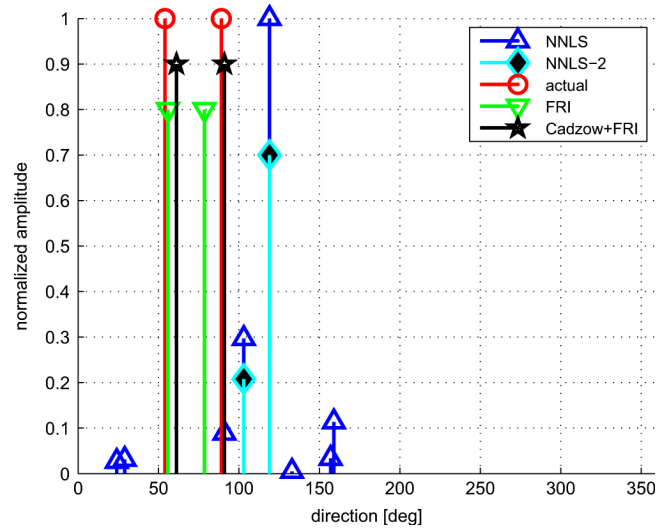
Fig. 14.   Experimental results from semi-outdoor experiment.

Fig. 13.   Experimental setup in a semi-outdoor propagation environment.
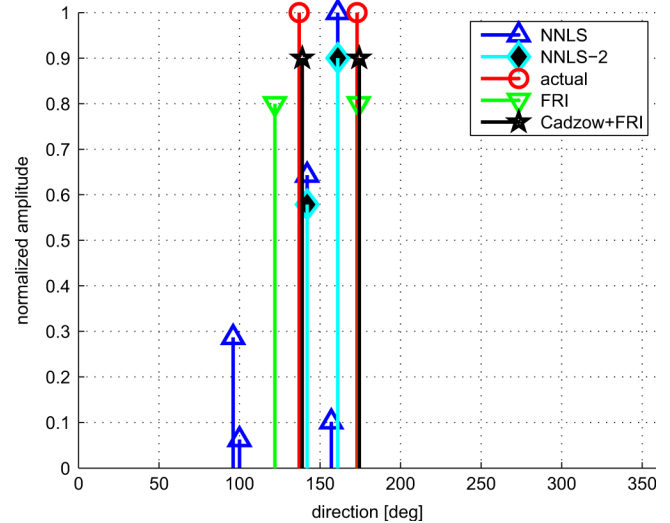
Fig. 15.   Experimental results from indoor experiment.

computed from 2560 discrete samples of the received signal are collected when the antenna's orientation is randomly changed. The transmitter is placed at 120° with respect to true north. The NNLS solution suffers from the present of spurious peaks which causes ambiguity in deciding which peak indicates the true DOA. This drawback can be overcome using the parametric methods. This is shown from the estimation result using the FRI and FRI with Cadzow denoising. It is demonstrated here that the use of Cadzow denoising helps to improve the estimation accuracy.

Although the experiment in the anechoic chamber has demonstrated the feasibility of the proposed approach, conducting experiment in a more realistic propagation environment may help to capture more non-idealities of the signal propagation as compared to the experiment in the anechoic chamber. With this motivation, we conducted more experiments in two different propagation environments: a semi-outdoor propagation at fire engine access field between South Spine Academic Complex S2.1 and S2.2, Nanyang Technological University (shown in Fig. 13) and an indoor propagation setup at the foyer of Research Techno Plaza, Nanyang Technological University.

The first environment is considered as semi-outdoor due to the confined wall at the two-side of the experiment area. For these experiments, two transmitters are utilized.

As many as 30 and 16 power measurements are collected together with its receiving antenna orientation for the semi-outdoor and indoor experiments, respectively. The results are shown in Figs. 14 and 15. In both figures, it can be observed that the FRI with Cadzow denoising yields better accuracy.

VIII. CONCLUSION

We have demonstrated using simulations as well as experimental results the feasibility of the proposed single power measurements based DF. With the derived CRB, we also show that the performance of the proposed approach converges to the CRB. The proposed approach utilizes a linear transformation of the vector of power measurements into a vector of observations that is common in spectral analysis problem, which can be solved using Pisarenko's method. Due to the noise at the received signal, the proposed approach incorporates Cadzow

denoising algorithm that exploits the matrix rank and linear structure properties. The problem of estimating the DOA from the power measurements of single receiving antenna can also be seen as stream of Diracs sampling problem in *spatial* domain.

APPENDIX
DERIVATION OF (12)

In the following derivation, we assume that the received power is calculated according to (3). Given that the discrete samples of received signal $x_l(n)$ is contaminated with complex Gaussian distributed random variables as described in (11), we have

$$|x_l(n)|^2 = \text{Re}\{x_l(n)\}^2 + \text{Im}\{x_l(n)\}^2$$
$$= |\breve{s}_l(n)|^2 + |\eta(n)|^2 + 2w(n)$$

where $\breve{s}_l(n) = \sum_{k=1}^{K} g(\tilde{\theta}_l - \theta_k)s_k(n)$ and

$$w(n) = \text{Re}\{\breve{s}_l(n)\}\text{Re}\{\eta(n)\} + \text{Im}\{\breve{s}_l(n)\}\text{Im}\{\eta(n)\}.$$

The modulus of a complex Gaussian distributed random variable will result in a Rayleigh distributed random variable with parameter σ^2

$$|\eta(n)| \sim \text{Rayleigh}(\sigma^2).$$

Taking sum of the squares of $|\eta(n)|$ over N samples will transform the Rayleigh distribution to a Gamma distribution with parameter N and $2\sigma^2$:

$$\sum_{n=0}^{N-1} |\eta(n)|^2 \sim \Gamma(N, 2\sigma^2).$$

Because of the large value of N, the Gamma distribution can be approximated as a Gaussian distribution $\mathcal{N}(2N\sigma^2, 4N\sigma^4)$. Therefore, we have

$$\frac{1}{N}\sum_{n=0}^{N-1} |\eta(n)|^2 \sim \mathcal{N}\left(\frac{2\sigma^2, 4\sigma^4}{N}\right). \tag{19}$$

The cross term $w(n)$ is negligible since the signal is uncorrelated with the noise. From the received power expression in (1), we are able to split the expression according to its random variable contribution

$$\hat{p}_l = \breve{p}_l + \frac{1}{N}\sum_{n=0}^{N-1} |\eta(n)|^2 \tag{20}$$

where $\breve{p}_l = 1/N \sum_{n=0}^{N-1} |\breve{s}_l(n)|^2$. With the distribution definition given in (19), we can deduce the distribution of the received power.

$$\hat{p}_l \sim \mathcal{N}\left(\breve{p}_l + 2\sigma^2, \frac{4\sigma^4}{N}\right). \tag{21}$$

Note that (21) can also be derived given that the probability distribution satisfied by $|x_l(n)|$ is known as Ricean distribution (generalization of Rayleigh distribution).

REFERENCES

[1] R. Schmidt, "Multiple emitter location and signal parameter estimation," *IEEE Trans. Antennas Propag.*, vol. 34, no. 3, pp. 276–280, Mar. 1986.

[2] G. Bienvenu and L. Kopp, "Adaptivity to background noise spatial coherence for high resolution passive methods," in *Proc. IEEE Int. Conf. Acoustics, Speech, Signal Processing (ICASSP)*, Apr. 1980, vol. 5, pp. 307–310.

[3] B. D. Rao and K. V. S. Hari, "Performance analysis of root-MUSIC," *IEEE Trans. Acoust., Speech, Signal Process.*, vol. 37, no. 12, pp. 1939–1949, Dec. 1989.

[4] R. Roy, A. Paulraj, and T. Kailath, "Direction-of-arrival estimation by subspace rotation methods—ESPRIT," in *Proc. Int. Conf. Acoustics, Speech, Signal Processing (ICASSP)*, Apr. 1986, vol. 11, pp. 2495–2498.

[5] F. Gao and A. B. Gershman, "A generalized ESPRIT approach to direction-of-arrival estimation," *IEEE Signal Process. Lett.*, vol. 12, no. 3, pp. 254–257, Mar. 2005.

[6] C. P. Mathews and M. D. Zoltowski, "Eigenstructure techniques for 2-D angle estimation with uniform circular arrays," *IEEE Trans. Signal Process.*, vol. 42, no. 9, pp. 2395–2407, Sep. 1994.

[7] B. Friedlander and A. J. Weiss, "Eigenstructure methods for direction finding with sensor gain and phase uncertainties," in *Proc. Int. Conf. Acoustics, Speech, Signal Processing (ICASSP)*, Apr. 11–14, 1988, pp. 2681–2684.

[8] P. Stoica and A. Nehorai, "MUSIC, maximum likelihood, and Cramer-Rao bound: Further results and comparisons," *IEEE Trans. Acoust., Speech, Signal Process.*, vol. 38, no. 12, pp. 2140–2150, Dec. 1990.

[9] M. Kaveh and A. Barabell, "The statistical performance of the MUSIC and the minimum-norm algorithms in resolving plane waves in noise," *IEEE Trans. Acoust., Speech, Signal Process.*, vol. 34, no. 2, pp. 331–341, Apr. 1986.

[10] A. L. Swindlehurst and T. Kailath, "A performance analysis of subspace-based methods in the presence of model errors. I. The MUSIC algorithm," *IEEE Trans. Signal Process.*, vol. 40, no. 7, pp. 1758–1774, Jul. 1992.

[11] P. Stoica, M. Cedervall, and T. Soderstrom, "Adaptive instrumental variable method for robust direction-of-arrival estimation," *Proc. Inst. Elect. Eng.—Radar, Sonar, Navigat.*, vol. 142, no. 2, pp. 45–53, Apr. 1995.

[12] A. Johansson and S. Nordholm, "Robust acoustic direction of arrival estimation using root-SRP-PHAT, a realtime implementation," in *Proc. IEEE Int. Conf. Acoustics, Speech, Signal Processing (ICASSP)*, Mar. 18–23, 2005, vol. 4, pp. IV/933–IV/936.

[13] A. Ferreol, P. Larzabal, and M. Viberg, "On the asymptotic performance analysis of subspace DOA estimation in the presence of modeling errors: Case of MUSIC," *IEEE Trans. Signal Process.*, vol. 54, no. 3, pp. 907–920, Mar. 2006.

[14] M. Rubsamen and A. B. Gershman, "Direction-of-arrival estimation for nonuniform sensor arrays: From manifold separation to Fourier domain MUSIC methods," *IEEE Trans. Signal Process.*, vol. 57, no. 2, pp. 588–599, Feb. 2009.

[15] B. C. Ng and A. Nehorai, "Optimum active array shape calibration," in *Conf. Rec. 25th Asilomar Conf. Signals, Systems, Computers*, Nov. 4–6, 1991, pp. 893–897.

[16] B. C. Ng and C. M. S. See, "Sensor-array calibration using a maximum-likelihood approach," *IEEE Trans. Antennas Propag.*, vol. 44, no. 6, pp. 827–835, Jun. 1996.

[17] B. P. Ng, J. P. Lie, M. H. Er, and A. Feng, "A practical simple geometry and gain/phase calibration technique for antenna array processing," *IEEE Trans. Antennas Propag.*, vol. 57, no. 7, pp. 1963–1972, Jul. 2009.

[18] J. Sheinvald and M. Wax, "Direction finding with fewer receivers via time-varying preprocessing," *IEEE Trans. Signal Process.*, vol. 47, no. 1, pp. 2–9, Jan. 1999.

[19] S. L. Preston, D. V. Thiel, J. W. Lu, S. G. O'Keefe, and T. S. Bird, "Electronic beam steering using switched parasitic patch elements," *Electron. Lett.*, vol. 33, no. 1, pp. 7–8, Jan. 1997.

[20] S. L. Preston, D. V. Thiel, T. A. Smith, S. G. O'Keefe, and J. W. Lu, "Base-station tracking in mobile communications using a switched parasitic antenna array," *IEEE Trans. Antennas Propag.*, vol. 46, no. 6, pp. 841–844, Jun. 1998.

[21] S. Zhang, G. H. Huff, J. Feng, and J. T. Bernhard, "A pattern reconfigurable microstrip parasitic array," *IEEE Trans. Antennas Propag.*, vol. 52, no. 10, pp. 2773–2776, Oct. 2004.

[22] O. Akhdar, D. Carsenat, C. Decroze, and T. Monediere, "A simple technique for angle of arrival measurement," in *Proc. Antennas and Propagation Soc. Int. Symp. (AP-S) 2008*, Jul. 5–11, 2008, pp. 1–4.

[23] O. Akhdar, M. Mouhamadou, D. Carsenat, C. Decroze, and T. Monediere, "A new CLEAN algorithm for angle of arrival denoising," *IEEE Antennas Wireless Propag. Lett.*, vol. 8, no. 2009, pp. 478–481, 2009.

[24] M. Vetterli, P. Marziliano, and T. Blu, "Sampling signals with finite rate of innovation," *IEEE Trans. Signal Process.*, vol. 50, no. 6, pp. 1417–1428, Jun. 2002.

[25] H. Krim and M. Viberg, "Two decades of array signal processing research: The parametric approach," *IEEE Signal Process. Mag.*, vol. 13, no. 4, pp. 67–94, Jul. 1996.

[26] M. Doron and E. Doron, "Wavefield modeling and array processing I. Spatial sampling," *IEEE Trans. Signal Process.*, vol. 42, no. 10, pp. 2549–2559, Oct. 1994.

[27] M. Doron and E. Doron, "Wavefield modeling and array processing. II. Algoritms," *IEEE Trans. Signal Process.*, vol. 42, no. 10, pp. 2560–2570, Oct. 1994.

[28] M. Doron and E. Doron, "Wavefield modeling and array processing. III. Resolution capacity," *IEEE Trans. Signal Process.*, vol. 42, no. 10, pp. 2571–2580, Oct. 1994.

[29] F. Belloni, A. Richter, and V. Koivunen, "DoA estimation via manifold separation for arbitrary array structures," *IEEE Trans. Signal Process.*, vol. 55, no. 10, pp. 4800–4810, Oct. 2007.

[30] P. Koivisto, "Reduction of errors in antenna radiation patterns using optimally truncated spherical wave expansion," *Progress Electromagn. Res.*, vol. 47, pp. 313–333, 2004.

[31] T. Blu, P.-L. Dragotti, M. Vetterli, P. Marziliano, and L. Coulot, "Sparse sampling of signal innovations," *IEEE Signal Process. Mag.*, vol. 25, no. 2, pp. 31–40, 2008.

[32] J. A. Cadzow, "Signal enhancement-A composite property mapping algorithm," *IEEE Trans. Acoust., Speech, Signal Process.*, vol. 36, no. 1, pp. 49–62, Jan. 1988.

[33] M. Wax and T. Kailath, "Detection of signals by information theoretic criteria," *IEEE Trans. Acoust., Speech, Signal Process.*, vol. 33, no. 2, pp. 387–392, Apr. 1985.

[34] B. Porat and B. Friedlander, "Computation of the exact information matrix of Gaussian time series with stationary random components," *IEEE Trans. Acoust., Speech, Signal Process.*, vol. 34, no. 1, pp. 118–130, Feb. 1986.

[35] P. Stoica and N. Arye, "MUSIC, maximum likelihood, and Cramer-Rao bound," *IEEE Trans. Acoust., Speech, Signal Process.*, vol. 37, no. 5, pp. 720–741, May 1989.

[36] C. L. Lawson and R. J. Hanson, *Solving Least Squares Problems*, ser. Prentice-Hall Ser. in Automatic Computation, C. L. Lawson and R. J. Hanson, Eds., 3rd ed.   Englewood Cliffs, NJ: Prentice-Hall, 1995.

[37] R. G. Baraniuk, "Compressive sensing (lecture notes)," *IEEE Signal Process. Mag.*, vol. 24, no. 4, pp. 118–121, Jul. 2007.

[38] WINRADIO WR-G305e Receiver WINRADIO [Online]. Available: http://www.winradio.com/home/g305e.htm

[39] Red Rapids: Pocket Change (PCMCIA) RedRapids [Online]. Available: http://www.redrapids.com/Products/PocketChange.aspx

[40] OceanServer, Ocean Server Digital Compass Products Digital Compass Products [Online]. Available: http://www.ocean-server.com/compass.html

Joni Polili Lie (M'09) received the B.Eng. and Ph.D. degrees in electrical and electronic engineering from Nanyang Technological University, Singapore, in 2004 and 2008, respectively.

He is currently a Research Scientist with the Sensor Array Research Programme, Temasek Laboratories, Nanyang Technological University, Singapore. His research interests include robust adaptive beamforming, parsimonious direction finding, impulse radio ultrawideband (UWB) array systems, and array signal processing in general.

Dr. Lie serves as reviewer for several international peer-reviewed journals.

Thierry Blu (M'96–SM'06) was born in Orléans, France, in 1964. He received the Diplôme d'ingénieur from the École Polytechnique, France, in 1986 and from the Télécom Paris (ENST), France, in 1988 and the Ph.D. degree in electrical engineering from ENST in 1996 for a study on iterated rational filterbanks, applied to wideband audio coding.

Between 1998 and 2007, he was with the Biomedical Imaging Group at the Swiss Federal Institute of Technology (EPFL), Lausanne, Switzerland. He is currently a Professor in the Department of Electronic Engineering, The Chinese University of Hong Kong. His research interests focus on (multi)wavelets, multiresolution analysis, multirate filterbanks, interpolation, approximation and sampling theory, sparse sampling, image denoising, psychoacoustics, biomedical imaging, optics, and wave propagation.

Dr. Blu was the recipient of two Best Paper Awards from the IEEE Signal Processing Society (in 2003 and 2006). He is also coauthor of a paper that received a Young Author Best Paper Award in 2009 from the same society. Between 2002 and 2006, he was an Associate Editor for the IEEE TRANSACTIONS ON IMAGE PROCESSING and, since 2006, for the IEEE TRANSACTIONS ON SIGNAL PROCESSING. He is also Associate Editor of Elsevier's *Signal Processing* and the *EURASIP Journal on Image and Video Processing*.

Chong Meng Samson See (M'92) was born in Singapore on June 13, 1968. He received the Diploma degree in electronics and communications engineering (with merit) from Singapore Polytechnic in 1988 and the M.Sc. degree in digital communication systems and the Ph.D. degree in electrical engineering, both from the Loughborough University of Technology, Loughborough, U.K., in 1991 and 1999, respectively.

Since 1992, he has been with DSO National Laboratories, Singapore, where he is now a Distinguished Member of Technical Staff and is currently leading a team in the research and development of advanced array signal processing systems and algorithms. He also holds an adjunct appointment at Temasek Laboratories, Nanyang Technological University, as a Principal Research Scientist, where he leads a program on sensor array research. His research interests include the area of statistical and array signal processing, communications, and bio-inspired systems. He has two issued patents on direction finding.

Dr. See is an Associate Editor of the IEEE TRANSACTIONS ON SIGNAL PROCESSING and a member of the IEEE Sensor Array and Multichannel Signal Processing Technical Committee.